Solar-Terrestrial Physics. 2024. Vol. 10. Iss. 2. P. 93–101. DOI: 10.12737/stp-102202409. © 2024
S.N. Ponomarchuk, V.I. Kurkin, N.V. Ilyin, M.S. Penzin. Published by INFRA-M Academic Publishing House

621.371.3, 537.87
DOI: 10.12737/stp-102202409

Received February 15, 2024
Accepted May 06, 2024

HF RADIO PATH MODELING BY WAVEGUIDE APPROACH

S.N. Ponomarchuk
Institute of Solar-Terrestrial Physics SB RAS, Irkutsk, Russia, spon@iszf.irk.ru

V.I. Kurkin
Institute of Solar-Terrestrial Physics SB RAS, Irkutsk, Russia, kurkin@iszf.irk.ru

N.V. Ilyin
Institute of Solar-Terrestrial Physics SB RAS, Irkutsk, Russia, ilyin@iszf.irk.ru

M.S. Penzin
Institute of Solar-Terrestrial Physics SB RAS, Irkutsk, Russia, penzin.maksim@gmail.com

Abstract. We present a scheme for modeling HF radio signal characteristics along paths of different lengths, which is based on the waveguide approach — the normal mode method. We use a representation of the recorded signal field in the form of Green function products of the angular operator, excitation coefficients, and reception coefficients of individual normal modes. Algorithms have been developed for calculating distance-frequency, frequency-angular, and amplitude characteristics of signals in large spatial regions through analysis and numerical summation of normal mode series. We have implemented a complex algorithm for simulating propagation conditions of HF radio signals, which includes a medium model, algorithms for calculating signal characteristics, and operational diagnostics of radio channel. We have compared the results of the HF signal propagation characteristic modeling and the experimental oblique sounding data obtained along paths of different lengths and orientation. To analyze experimental ionograms, determine the maximum usable frequencies for propagation modes along radio paths, we employ the method of automatic processing and interpretation of oblique sounding ionograms.

Keywords: radio wave propagation, waveguide approach, radio path forecast, ionogram, radio channel diagnostics.

INTRODUCTION

Efficiency of radio systems, including cognitive radio, depends on the quality and promptness of adjustment of system parameters through active and passive ionospheric sounding [Anderson, 2019; Ayliffe et al., 2019]. When using oblique sounding (OS) data to adapt parameters of radio systems, in particular, to determine the range of operating frequencies, it is necessary to predict in real time radio signal characteristics in order to interpret results of sounding in the selected HF radio paths. Identifying frequency dependences group delays of propagation modes in recorded ionograms makes it possible to estimate dispersion distortions of a signal in a radio channel for their further elimination when processing radio signals in a receiver consistently with the emitted signal [Ivanov et al., 2019a, b].

The existing methods of modeling HF radio paths are mainly based on the geometrical optics method [Kazantsev et al., 1967; Lukin, Spiridonov, 1969; Kravtsov, Orlov, 1980; Croft, Hoogasian, 1968; Kelso, 1968; Haselgrove, 1957; Mullaly, 1962; Rao, 1968]. The calculation methods developed in the early 70s can carry out a trajectory synthesis of field distribution over space and estimate the signal field amplitude. To more accurately describe radio wave propagation in inhomogeneous magnetically active media in view of peculiarities in the caustic region, methods of Maslov canonical operator and the theory of catastrophes are employed [Ipatov et al., 1990, 2014; Kryukovskii et al., 2006]. The influence of random irregularities of different scales was studied using the interference integral method [Avdeev et al., 1988] and the generalized Rytov method [Zernov et al., 1992]. The parabolic equation method was also employed [Cherkashin, 1971; Baranov, Popov, 1993]. The adiabatic invariant method [Gurevich, Tsedilina, 1979] and its generalization based on asymptotic solutions of ray equations [Baranov et al., 1992] have increased the efficiency in the analysis of long-distance radio paths. To study radio signal propagation in dispersion media, a method for space-time geometrical theory of diffraction was developed [Anyutin, Orlov, 1977].

One of the methods for describing HF radio signal propagation is the waveguide approach — the normal mode method [Krasnushkin, 1947; Bremmer, 1949; Kurkin et al., 1981a]. Within the framework of this approach, a complex model of HF radio channel has been built which includes a transmitter and a receiver, antenna-feeder systems, the Earth—ionosphere waveguide, and a software package for calculating radio signal characteristics [Kurkin et al., 2023]. A representation of the transfer function of radio channel was obtained in the form of a series of products of angular-operator Green functions, excitation coefficients, and reception coefficients of individual normal modes for TM and TE fields. The scheme for solving the radial problem and constructing spectrum of the radial operator has been modified with regard to signal field absorption in the ionosphere and on Earth's surface. This allows us to model the HF radio channel in the frequency range including frequencies below the F2-layer critical frequency. From analysis and numerical summation of a number of normal modes, algorithms have been developed

for calculating distance-frequency (DFC), frequency-angular, and amplitude characteristics of signals, including time sweep. Radio signal characteristics are calculated for transmitted signal modulation of different types in view of signal processing in the receiver. A feature of the algorithms is the determination of normal mode characteristics throughout the radio path with a given range increment, which enables the use of the function approximation for calculating signal field characteristics at any point of the path. In this study, which is a sequel to the work [Kurkin et al., 2023], we present the results of comparison between HF radio path characteristics, calculated by the developed radio channel model, and experimental OS data, obtained by the ISTP SB RAS multifunction chirp ionosonde [Podlesnyi et al., 2013]. To model the HF radio signal characteristics and diagnose the radio channel, we have implemented a software package that includes ionosphere and underlying surface models, a database of transmitting and receiving antennas, and blocks for calculating signal characteristics. To analyze experimental ionograms and determine maximum usable frequencies (MUFs) of propagation modes along a radio path, a method for automatic processing and interpretation of OS ionograms is used [Grozov et al., 2012; Ponomarchuk, Grozov, 2023].

RADIO WAVE PROPAGATION MODEL

Let us examine a numerical scheme for modeling HF radio path characteristics, using a sounding pulse signal as an example. The expression for the recorded signal in a receiver, located at a point $\vec{r} = (r, \theta, \varphi_F)$, can be written as a series of products of angular-operator Green functions, excitation coefficients, and reception coefficients of individual normal modes [Kurkin et al., 2023]

$$u_a(\vec{r}, t) = w(\vec{r}, t) e^{iW(\vec{r}, t)} = \\ = \mathrm{Re} \sum_{n=n_1}^{n=n_m} \left[a_n(\vec{r}, \omega_0) g_0(t - \tau_n(\theta)) e^{i\Psi_n(\theta, \omega_0)} \right] e^{-i\omega_0 t}. \quad (1)$$

Here, $a_n(\vec{r}, \omega_0) = A_n \left[\tilde{D}_n^e(\varphi) \tilde{P}_n^e(\varphi_F) + \tilde{D}_n^m(\varphi) \times \right.$ $\left. \times \tilde{P}_n^m(\varphi_F) \right] e^{-\Gamma_n(\theta)}$ is the amplitude factor of the normal mode; $A_n = -i \dfrac{\sqrt{2\pi ka}}{c\sqrt{\gamma_n \sin\theta}} e^{i\frac{\pi}{4}}$; $g_0(t)$ is the transmitted pulse envelope; $\tau_n(\theta) = \int_0^\theta \dfrac{dka\gamma_n}{d\omega} d\theta'$ is the delay in the normal mode for a given range θ; $\Psi_n(\theta, \omega_0) = ka \int_0^\theta \gamma_n(\theta') d\theta'$ is the wave phase; $k = \omega_0/c$; a is the Earth radius; $\Gamma_n(\theta) = ka \int_0^\theta \left[\left(\nu_n^e + \nu_n^m \right)/2 \right] d\theta'$ is normal mode attenuation; γ_n and $\nu_n^{e,m}$ are the real and imaginary parts of the spectral parameter $\tilde{\gamma}_n^{e,m}$. The polar axis of the spherical coordinate system is assumed to pass through the location of the transmitter. A scheme for constructing series of normal modes (1) in the inhomogeneous azimuthally symmetric Earth—ionosphere waveguide is given in [Kurkin et al., 2023]. Within the framework of the cross-sectional method, the waveguide is subdivided into uniform comparison waveguides [Popov, Potekhin, 1984], each with a radial boundary value problem formulated. The solution of the second-order equation for electromagnetic field components is sought as eigenfunction $R_n^{e,m}(r, \theta)$ expansion of radial boundary value problems for the comparison waveguides. The variable separation method is employed to obtain waveguide equations for the coefficients of field expansion into a series, which are solved without regard to the interaction between normal modes during the transition from one comparison waveguide to another. On the assumption of a smooth change in the ionospheric parameters depending on the angular coordinate θ, we find the solution of the waveguide equations in the adiabatic approximation, using the standard-equation method. In this approximation, the normal mode number n is an adiabatic invariant. At each point of the radio path, we can therefore use solutions of the radial problem for the spherically symmetric model of the Earth—ionosphere waveguide with respective medium parameters to determine eigenvalues $\left(\tilde{\gamma}_n^{e,m}\right)^2$ and eigenfunctions $R_n^{e,m}(r, \theta)$ for a given n. Thus, the spectral parameter $\tilde{\gamma}_n^{e,m}(\theta)$ can be considered a function of the angular coordinate θ. The normal mode characteristics $\Psi_n(\theta, \omega_0)$, $\tau_n(\theta)$, and $\Gamma_n(\theta)$ are determined by the integral functions of the angular coordinate θ and depend on properties of the propagation medium.

Amplitude factors of normal modes include the excitation $\tilde{D}_n^{e,m}$ and reception $\tilde{P}_n^{e,m}$ coefficients of TM- and TE-type normal modes, which are calculated for specified antenna-feeder devices [Kurkin et al., 2023]. Note also that expression for recorded signal (1) was obtained in the isotropic Earth—ionosphere waveguide regardless of the magnetic field, so the sounding wave polarization type is not determined. The magnetic field is taken into account phenomenologically by introducing an effective index of signal energy absorption in the waveguide $\tilde{\nu} = \left(\nu_n^e + \nu_n^m\right)/2$ in the exponent in the expression for the amplitude factor of the normal mode [Kurkin et al., 1981b]. The magnetic-ionic separation of signals is ignored, which determines the choice of the normal mode phase in (1).

Limits of summation in (1) are selected from the conditions of effective excitation of normal modes n_1 and low attenuation of modes due to absorption or penetration of modes through the ionosphere n_m. The numbers n_1 and n_m are calculated using the equation of normal-mode spectrum from the boundary values of the real part of the radial problem eigenvalue $\xi_n = \gamma_n^2 - \nu_n^2$, which define the group of normal modes forming the field of a signal in the waveguide [Kurkin et al., 2023]. Boundary values of ξ_n are

found from the equality defining WKB singular points — the solutions for the radial-operator eigenfunctions — turning (reflection) points. For a given electron density profile $N_e(r)$ [m^{-3}], this equality has the form

$$\xi_n = \left(\frac{r}{a}\right)^2 \left[1 - \frac{80.6 N_e(r)}{f^2}\right]. \quad (2)$$

The ground-based transmitter located at $\vec{r}_b = (b, 0, \varphi)$ effectively excites normal modes with $n > n_1(0)$, where $n_1(0)$ is calculated at $\gamma_n = b/a$, which determines the lower turning point of the WKB solution for $\gamma_n > 1$ [Kurkin et al., 2023]. On the other hand, the resulting current at the output of the receiving antenna at $\vec{r} = (r, \theta, \varphi_F)$ depends on modes with $n > n_1(\theta)$, where $n_1(\theta)$ is calculated from the spectrum equation at $\gamma_n = r/a$. The normal modes, whose spectral parameter $\gamma_n > r/a$, do not participate in the formation of current in the antenna since the field strengths of these modes near the receiving antenna are low [Kurkin et al., 1981a]. Thus, the lower limit of summation $n_1 = \max\left[n_1(0), n_1(\theta)\right]$.

To select the upper limit of summation in (1), we examine the conditions for the existence of the radio wave propagation waveguide channel made up by Earth's surface and the ionospheric E, F1, or F2 layer. Local minima and points of inflexion of ξ_n for the given angular coordinate θ are responsible for the parameters $\xi^j_{\min}$ and $\xi^j_{\max}$, where $j = 1$, 2, 3 for E, F1, and F2 respectively. The values of $\xi^j_{\min}$ and $\xi^j_{\max}$ for the waveguide channel are selected from the condition of the existence of turning points in an ionospheric layer. Using the normal wave spectrum equation, we can calculate the corresponding lower and upper boundary numbers n^j_1 and n^j_m in the waveguide channel from $\xi^j_{\max}$ and $\xi^j_{\min}$. In the inhomogeneous waveguide, $\xi^j_{\min}(\theta)$ and $\xi^j_{\max}(\theta)$ change along the radio path, thereby causing the transition of normal modes from one waveguide channel to another, the transition to an interlayer channel, or wave leakage through the ionosphere. The value $\xi^1_{\max}(0) = b/a$ or $\xi^1_{\max}(\theta) = r/a$ is taken as $\xi^1_{\max}$ on the radio path. The implemented algorithm for calculating HF signal characteristics takes into account only those normal mode groups that propagate in the waveguide channels existing throughout the radio path, without transitions and leakage. Boundaries of the mode groups in each waveguide channel are defined as $\max n^j_1(\theta_1)$ and $\min n^j_m(\theta_1)$, where $0 < \theta_1 < \theta$. Thus, the complete normal mode group, which forms the current in the receiving antenna, is a combination of groups of normal modes propagating in the waveguide of the E, F1, and F2 layers. For the upper limit of the number for the complete group of normal modes forming the signal field at the receiving point we can take $n_0 = \min n^3_m(\theta_1)$, where $0 < \theta_1 < \theta$. The normal modes with $n > n_0$ penetrate through the ionosphere when propagating along the radio path, i.e. they do not have reflection points. For low radiation frequencies lower than the F2-layer critical frequency along the radio path, the spectral parameter $\gamma_{\min}$ corresponding to $\xi^3_{\min}$ tends to zero and n_0 grows. At the same time, the imaginary part of the spectral parameter $\nu_{\min}$ increases sharply, thereby leading to a strong attenuation of the signal already at short distances from the transmitter. For example, the radiation field decreases e times at a distance d=10 km for f=3 MHz [Kurkin et al., 2023]. Therefore, in the implemented algorithm for calculating signal characteristics for low radiation frequencies, we choose $\xi^3_{\min} \cong -10^{-4}$, from which the upper limit of summation in (1) is calculated. Signal characteristics along inhomogeneous radio paths for a ground transmitter and receiver are, in fact, calculated for separate waveguide propagation channels with the boundaries of normal mode groups n_1 and $n^j_0 = \min n^j_m(\theta_1)$, where $0 < \theta_1 < \theta$.

Determining the boundary numbers $n_1 = \max\left[n_1(0), n_1(\theta)\right]$ and n_0 depending on ionospheric parameters allows us to calculate an important characteristic of radio wave propagation — the limiting frequency of radio communication in the Earth—ionosphere waveguide for a given angular distance and heights of the transmitting and receiving antennas above Earth's surface [Kurkin et al., 1975]. As the radiation frequency increases, n_1 grows and n_0 decreases. The equality

$$n_1 = \max\left[n_1(0), n_1(\theta)\right] = n_0 \quad (3)$$

defines the upper limit of the frequency range to search for MUF of the radio path.

The field of a single normal mode is distributed throughout the waveguide section and depends on its global characteristics. The total field of a signal is localized in the waveguide regions, where the stationary condition of individual mode groups holds — the phase difference between adjacent normal modes is a multiple of 2π [Potekhin, Orlov, 1981]. For the ground-based transmitter and receiver, the stationary condition of individual mode groups has the form

$$\Delta\Psi_n(\theta) = (\Psi_n - \Psi_{n+1}) = 2\pi l, \quad (4)$$

where l is an integer. Equation (4) determines the numbers of central modes of the groups of phased normal modes that make the main contribution to the field of a signal at the receiving point. The spectral parameter of the central mode of the phased mode group with the number n_i can be related to the elevation angle ϕ_1 for the path from the transmission point with the radial coordinate b by the ratio $\cos\phi_1 = a\gamma_{n_i}(0)/b$ [Kurkin et al., 1981a]. In the spherically symmetric waveguide, stationarity equation (4) can be reduced to the expression for the jump distance along Earth's surface [Dyson, Bennett, 1988], using the relationship between ϕ_1 and γ_n,

$$D = 2a^2 \cos\phi_1 \int_a^{r_n} \frac{dr}{r\sqrt{\varepsilon r^2 - a^2\cos^2\phi_1}}. \quad (5)$$

Here r_n is the reflection point of the ray in the ionosphere. Then, l in (4) is the number of reflections of the signal field from the ionosphere.

The numerical solution of transcendental equation of stationarity (4) with respect to the angular distance θ for given values of n_i allows us to plot the dependence $D(n_i) = a\theta(n_i)$ analogous to the variation of range with angle $D(\phi_1)$. Calculating the group delay of the central mode n_i and using $\theta(n_i)$, we obtain the dependence $P(n_i)$ — an analog of the variation of group path with angle $P(\phi_1)$, where P is the group path. The central numbers n_i are transformed to ϕ_1, using the relation between n_i and the spectral parameter γ_{n_i} by the equation for the normal wave spectrum [Kurkin et al., 2023]. Separate dependences $D^j(\phi_1)$ and $P^j(\phi_1)$ are found for each of the E, F1, and F2 waveguide channels. For given f and D for each channel, there are two solutions of (4) with respect to the elevation angle for the path from the transmission point, which correspond to the lower and upper rays [Davies, 1973]. As distance decreases at a given frequency f, the propagation paths corresponding to the lower and upper rays approach each other and intersect at a minimum point in $D^j(\phi_1)$. The minimum point corresponds to the skip zone border D_m^j. For D_m^j, f is propagation mode MUF f_m^j. The minimum in $P^j(\phi_1)$ defines the minimum group path P_m^j. The distance to the skip zone border D_m^j does not coincide with the distance at which P_m^j is obtained. With an increase in the operating frequency, this difference decreases. The frequency dependences $D_m^j(f)$ and $P_m^j(f)$ are calculated to analyze and interpret BS ionograms by a continuous chirp signal [Ponomarchuk et al., 2022].

Propagation mode MUFs and skip zone borders along Earth's surface for each of the E, F1, and F2 waveguide channels can be promptly determined by solving the equation

$$\max_{n\in[n_1,\,n_m]} \Delta\Psi_n(\theta,\, f) = l. \tag{6}$$

Solving this equation with respect to f for a given distance $D=a\theta$ determines MUF of l. Solving Equation (6) with respect to θ for given f yields the distance to the skip zone border of the lth jump.

Expressions (1), (4), and (6) serve as a formula basis of the scheme for calculating the distribution of the HF signal field in the Earth—ionosphere waveguide by the normal mode method. At the first stage, the normal mode characteristics a_n, Ψ_n, τ_n, $\Delta\Psi_n$ are calculated at spectral reference points from given electron density profiles $N(r)$ and the effective collision frequency $\rho_{eff}(r)$ at selected points of the radio path. The normal mode groups forming the signal field at the receiving point for the E, F1, and F2 waveguide channels are identified. Numerical studies have shown that in smoothly irregular waveguides the normal mode characteristics smoothly change depending on the number n at a given coordinate θ and on θ at given n. This makes it possible to effectively use the function approximation for calculating a_n, Ψ_n, τ_n, $\Delta\Psi_n$ at intermediate points from n and θ in algorithms for calculating signal characteristics. To ensure sufficient accuracy in calculating the normal mode characteristics, it is enough to select 100 spectral reference points. The number of points for θ is determined by the interval of setting the profiles $N(r)$ and $\rho_{eff}(r)$ along the radio path. For long radio paths, the interval is 200–400 km.

At the second stage, solving (4) with respect to n_i allows us to determine for each of the E, F1, and F2 waveguide channels the mode structure of a signal (the number of signals and their identification) and calculate MUF, time and angular characteristics of signals for propagation modes. The number n_i is related to the angle of arrival of the path ϕ_2 at the receiving point by the ratio $\cos\phi_2 = a\gamma_{n_i}(\theta)/r$. In this way, we calculate the frequency-angular characteristic of recorded signals at the receiving point.

Amplitude characteristics of signals for each of the waveguide channels are calculated using (1). The envelope $w(\vec{r}, t)$ of the recorded signal in each waveguide channel is computed through direct numerical summation of expressions of the form [Kurkin et al., 1982]

$$w(\vec{r}, t) = \left[\left(\sum_{n=n_1}^{n=n_0^j} a_n g_0(t-\tau_n)\cos\Psi_n\right)^2 + \left(\sum_{n=n_1}^{n=n_0^j} a_n g_0(t-\tau_n)\sin\Psi_n\right)^2\right]^{1/2}. \tag{7}$$

The sum of normal modes is defined by the smooth dependence of the normal mode characteristics a_n, Ψ_n, τ_n on n, which enables us to implement the effective summation scheme with the function approximation in the calculations. In the case of a quasi-monochromatic pulse signal transmitted at the time t regardless of the effect of signal blurring, the value $w(\vec{r}, t)$ is determined by a group of modes whose group delays lie within the interval $[t-\tilde{T}, t]$ (the modes are present at t at the receiving site). Here, $\tilde{T}$ is the full pulse length. Then, the interval of numbers $[n_1, n_0^j]$ in (7) for calculating $w(\vec{r}, t)$ at t can be replaced by an interval $[n_H(t), n_k(t)]$, where n_H is the number of a mode whose delay for the distance θ considered is equal to $t-\tilde{T}$, and n_k is the mode number with $\tau_{n_k} = t$. According to (7), the summation at each moment of time is carried out over n with a step equal to 1; therefore, to reduce the computer time the calculation is organized as follows. The entire time sweep from τ_H to τ_k (τ_H and τ_k depend on the delays in the fastest and slowest waves from the interval $[n_1, n_0^j]$ respectively) is divided into $m = (\tau_k - \tau_H)/\Delta t$ intervals, where Δt is a given time step with $\Delta t<\delta$, where δ is

the pulse front time. Further, in the loop on $\left[n_1, n_0^j\right]$ for each normal mode, amplitude, phase, and delay are calculated and instants of time t_s are determined from $m+1$ time readings, when this mode participates in signal formation, from the condition $t_s - \tilde{T} \le \tau_n \le t_s$. Then, the real and imaginary parts of the normal mode with regard to the envelope (separate terms in (7)) are entered in respective elements of the arrays. At the end of the loop on the numbers, using the simplest arithmetic operations we obtain an array of envelope values $w(\vec{r}, t)$ at $m+1$ time sweep points. Calculation of the signal envelope $w(\vec{r}, t)$ allows us to examine the shape of the received signal both for time-separated pulses and for overlapping ones, i.e. both in the skip zone and in the caustic region, where the upper and lower rays merge [Kurkin et al., 2023]. The signal envelope in the center of the pulse of a signal corresponding to the delay in the central mode of a set of phased normal modes $\tau_{n_i} + \tilde{T}/2$, can be taken as the signal amplitude.

The developed scheme for calculating characteristics of pulsed signals is also applicable to characteristics of chirp signals if treated by the frequency compression method [Ivanov et al., 2003]. In this case, the result of processing of a time sample of the recorded chirp signal is equivalent to the passage of the narrow-band pulsed signal, whose characteristics are defined by the time window, through the radio channel [Ilyin et al., 1996; Podlesnyi et al., 2014].

ANALYSIS OF EXPERIMENTAL DATA

To simulate HF radio paths, a complex algorithm has been implemented which includes a medium model, algorithms for calculating signal characteristics and interpreting ionograms. Radio signal characteristics are calculated using complex arithmetic. To test the developed algorithms for modeling signal characteristics and interpreting ionograms, we have employed data from the OS radio path network covering northeastern Russia and created on the basis of the spatially distributed multifunctional chirp ionosonde developed at ISTP SB RAS [Podlesnyi et al., 2013]. Geometry of the paths is shown in Figure 1. Transmitting stations: Magadan (60° N, 150.7° E), Khabarovsk (47.6° N, 134.7° E), Norilsk (69.4° N, 88.4° E), Usolye-Sibirskoye (52.9° N, 103.3° E). Receiving station Irkutsk: Tory village, Buryatia (51.8° N, 103° E).

By solving transcendental equation (6), we have implemented an operational algorithm for calculating MUFs of various propagation modes along HF radio paths. Verification of the algorithm for predicting MUF of mode 1F2 from experimental maximum observed frequencies (MOFs) at the network of OS radio paths in northeastern Russia has demonstrated its effectiveness in various heliogeophysical conditions. Figure 2 illustrates diurnal variations in the MOF median (solid black line) for propagation mode 1F2 along the Magadan—Irkutsk path (3000 km) in July (*a*) and December (*b*) 2013. Vertical lines indicate intervals of MOF variations within a month. Also presented here are the results of the calculation of MUF of mode 1F2 by IRI–2016 [Bilitza et al., 2017] (dashed line). Standard deviations of the relative prediction error in July and December 2013 were 6.4 and 11 %.

Similar diurnal variations of the MOF median and calculated MUFs for propagation mode 1F2 along the Khabarovsk—Irkutsk path (2300 km) are shown in Figure 3 for July (*a*) and December (*b*) 2013. For the Khabarovsk—Irkutsk path, standard deviations of the prediction error were 5.4 and 11.2 % respectively in July and December 2013.

To analyze experimental data, determine MUFs, and construct signal tracks of individual propagation modes, an algorithm for automatic interpretation of OS ionograms has been implemented [Grozov et al., 2012; Ponomarchuk, Grozov, 2023]. It rests on the results of DFC

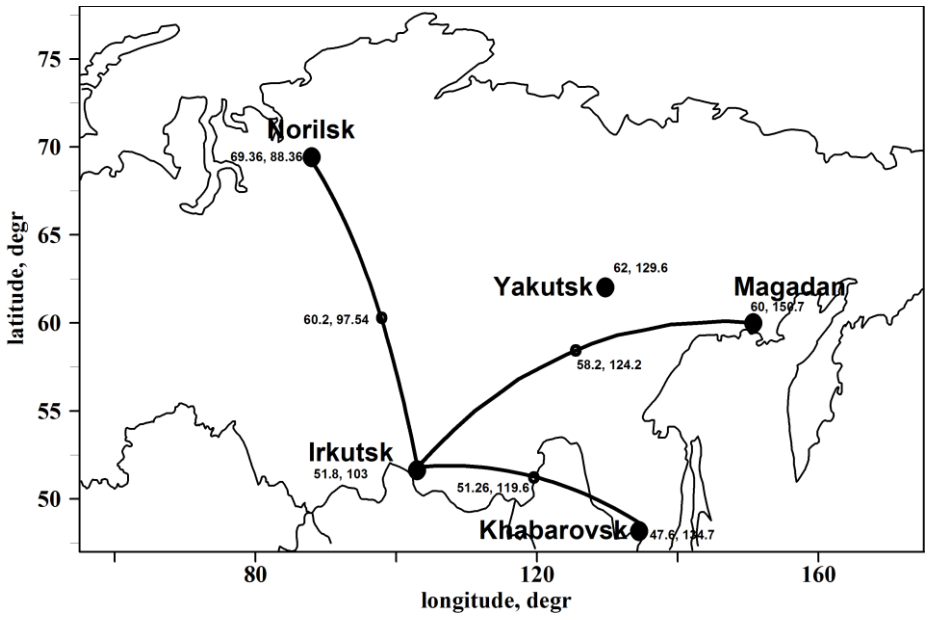

Figure 1. Geometry of OS paths in northeastern Russia

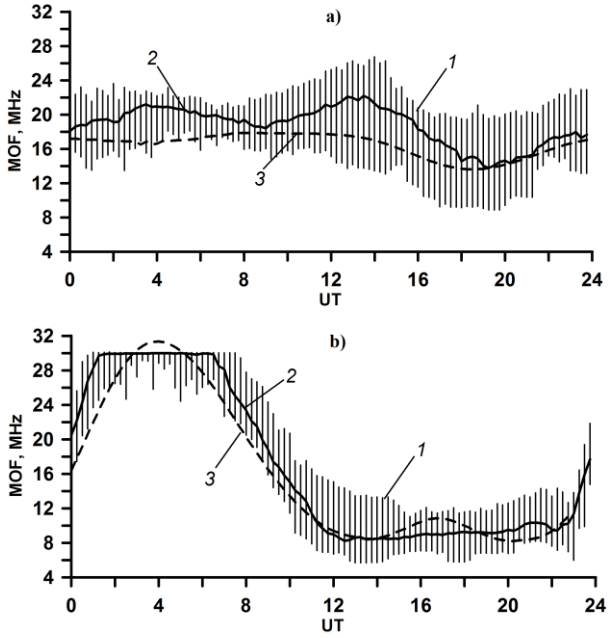

Figure 2. Diurnal variations in the MOF median and calculated MUF along the Magadan—Irkutsk path in July (*a*) and December (*b*) 2013: 1 — MOF variation intervals; 2 — MOF median; 3 — calculated MUFs

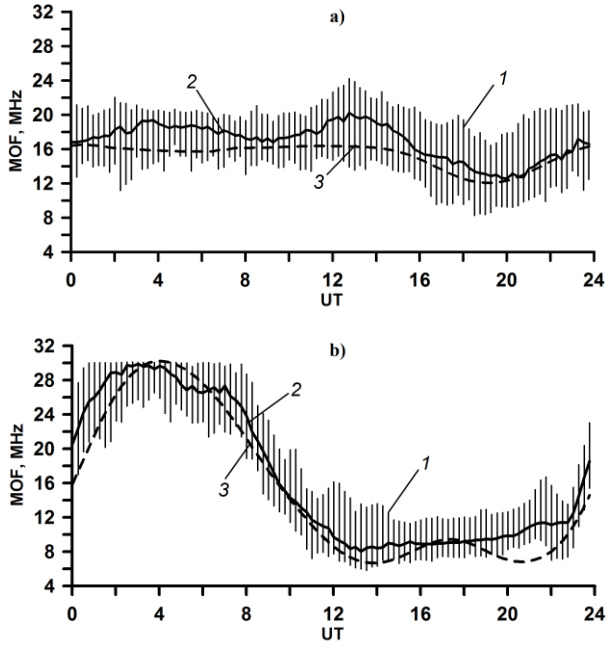

Figure 3. The same as in Figure 2 for the Khabarovsk—Irkutsk path

modeling along a given path in the long-term prediction mode, adiabatic invariants, and the results of secondary processing of the experimental ionogram — points with significant amplitude. The method is based on adiabatic invariants — values that persist during variations in ionospheric parameters within the accuracy of long-term prediction (20 %), namely:

- the ratio P_m/D of the group path P_m at the closing point of the lower and upper rays of the propagation mode to the radio path length D;
- the ratio between MUFs of modes of different multiplicities propagating in one of the waveguide channels χ;
- the frequency dependence of the group path P of the propagation mode in the normalized frequency grid $\beta=f/f_m$, where f_m is MUF of the mode for the distance $P(\beta)$ considered.

Based on the results of OS signal recording, an OS ionogram characterizing the frequency dependence of the group time of signal propagation is formed at the receiver output. In general, the ionogram is a matrix, where each element (amplitude) $A(f_i, P_j)$ is determined by two characteristics: group path (signal delay) P_j and frequency f_i. To isolate an array of points corresponding to the moments of arrival of signals with significant amplitude in the signal-to-noise ratio, secondary processing of the ionogram is carried out [Grozov et al., 2012]. An array of points with significant amplitude is formed $(f, P)_k$, $k=\overline{1, M}$. An algorithm for determining MUFs of propagation modes in the F1 and F2 waveguide channels has been developed based on a model mask constructed from the long-term prediction of DFC of OS along the radio path. The mask for the selected propagation mode moves without turning, by superposing the nose of the mask on the points with significant amplitude $(f, P)_k$, $k=\overline{1, M}$. The superposition is carried out in the normalized frequency grid β, recalculated at each step. The values of f_m^r and P_m^r, at which the number of points in the mask is maximum, are taken as real MUFs and the group path of the closing point of the propagation mode upper and lower rays. The results of determination of propagation mode MUFs are used to correct respective calculated DFC of OS signals. The rectangular mask was also employed to implement the algorithm for identifying signals reflected from the E_s layer. Figure 4, *a* presents the OS ionogram obtained along the Magadan—Irkutsk path on January 09, 2023 at 01:15 UT, and the results of modeling of OS DFC from the long-term prediction by IRI-2016. The error of the long-term prediction was ~30 %. Panel *b* shows the results of interpretation of the ionogram that allows us to identify the signals related to propagation modes 1F2, 2F2, and 3F2, and to correct predicted OS DFC of these modes.

Figure 5 presents the OS ionogram obtained from the Khabarovsk—Irkutsk path on January 09, 2023 at 01:11 UT and the results of interpretation of propagation modes 1F2 and 2F2. Figure 6 shows the OS ionogram obtained from the Norilsk—Irkutsk path (2088 km) on January 09, 2023 at 01:33 UT and the results of interpretation of propagation modes 1F2 and 2F2.

The above ionograms were obtained in winter in the absence of ionospheric disturbances and featured a fairly simple mode structure of received signals.

The main traces of reflections in the OS ionograms correspond to signals arriving at the receiving point through reflection from the F2 layer. The mode structure of the recorded signal becomes more complicated in the presence of large-scale ionospheric irregularities or traveling ionospheric disturbances (TIDs) along the radio wave propagation path [Kurkin et al., 2024]. In summer, the multilayer

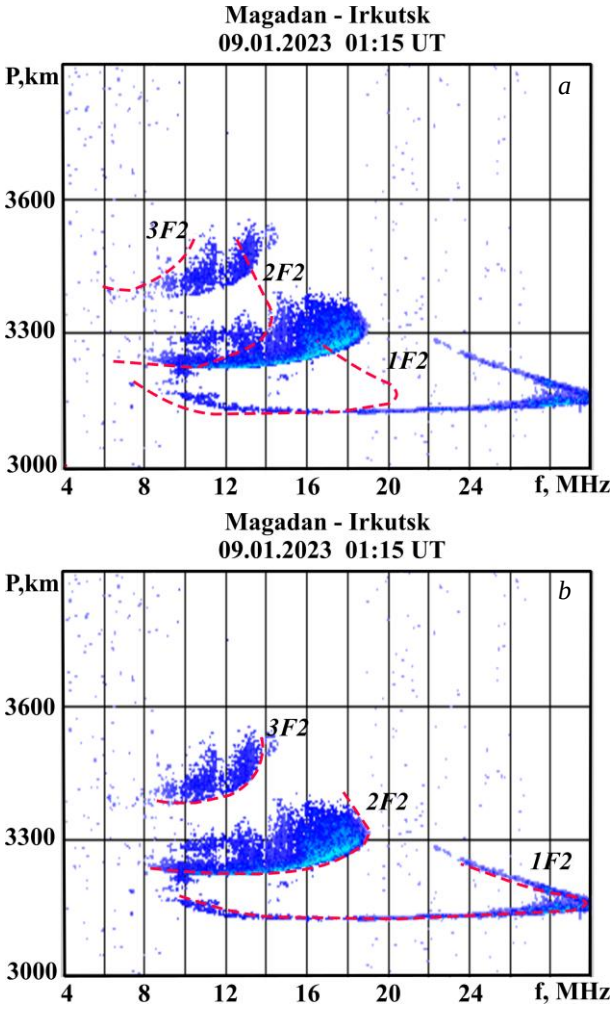

Figure 4. OS ionogram obtained from the Magadan—Irkutsk path on January 09, 2023 at 01:15 UT; results of DFC modeling (*a*) and interpretation of propagation modes (*b*)

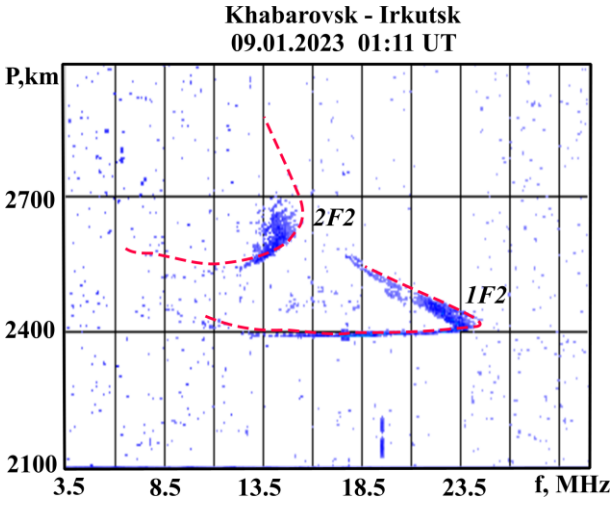

Figure 5. OS ionogram obtained from the Khabarovsk—Irkutsk path on January 09, 2023 at 01:11 UT and the results of interpretation of propagation modes

structure of the ionosphere leads to the appearance of additional signals reflected from the F1 layer in OS ionograms. A distinctive feature of summer daytime OS ionograms is the presence of pronounced traces corresponding to delays in the arrival of signals reflected from the E_s layer. During some summer daytime periods, the E_s layer becomes

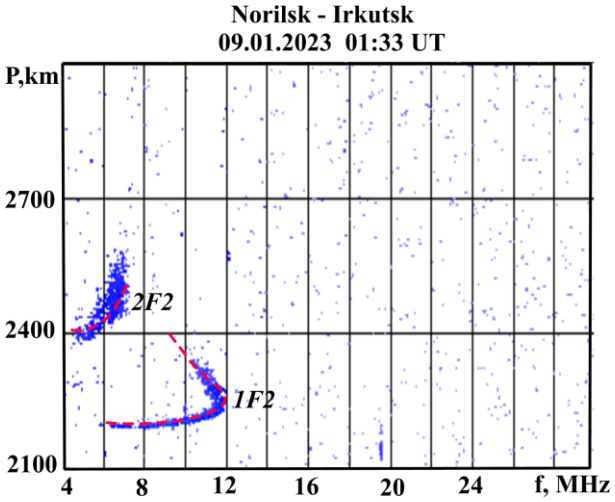

Figure 6. OS ionogram obtained from the Norilsk—Irkutsk path on January 09, 2023 at 01:33 UT and the results of interpretation of propagation modes

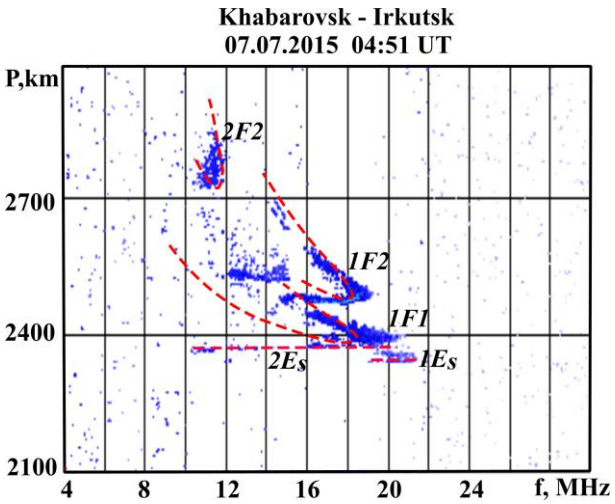

Figure 7. OS ionogram from the Khabarovsk—Irkutsk path on July 07, 2015 at 04:51 UT and the results of interpretation of propagation modes

dominant along the path, which results in complete shielding of the overlying reflecting F1 and F2 layers. The maximum operating frequency for receiving signals reflected from the E_s layer may exceed the maximum frequency of the transmitter. Figure 7 displays the OS ionogram obtained from the Khabarovsk—Irkutsk path on July 07, 2015 at 04:51 UT. Red dashed lines are the results of automatic interpretation of propagation modes 1F1, 1F2, and 2F2 and the results of interpretation of signals reflected from the E_s layer (modes $1E_s$ and $2E_s$).

The developed methods and algorithms for calculating and analyzing propagation characteristics are also applicable for modeling long HF radio paths. Figure 8 illustrates an OS ionogram obtained from the Cyprus—Irkutsk path (5650 km) on January 05, 2023 at 08:00 UT and the results of DFC interpretation. This path is in the middle latitudes. It can be seen that the ionogram interpretation algorithm makes it possible to identify propagation modes 2F2, 3F2, and 4F2 with subsequent correction of DFC.

Figure 9 shows the OS ionogram obtained from the Alice-Springs—Irkutsk transequatorial path (8937 km) on March 11, 1996 and the results of interpretation of propagation modes 3F2, 4F2, and 5F2.

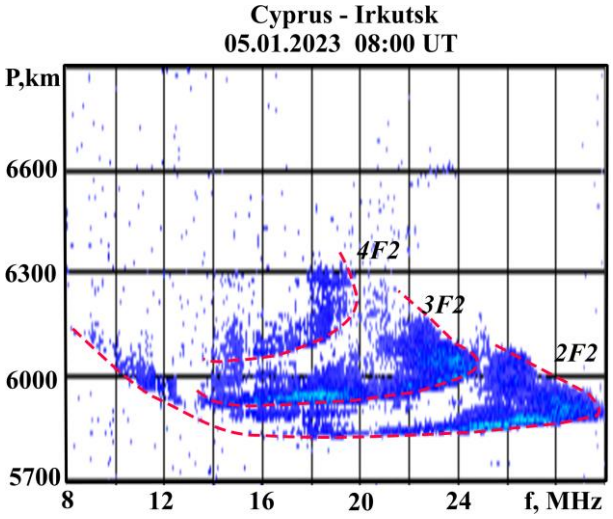

Figure 8. OS ionogram obtained from the Cyprus—Irkutsk path on January 05, 2023 at 08:00 UT and the results of interpretation of propagation modes

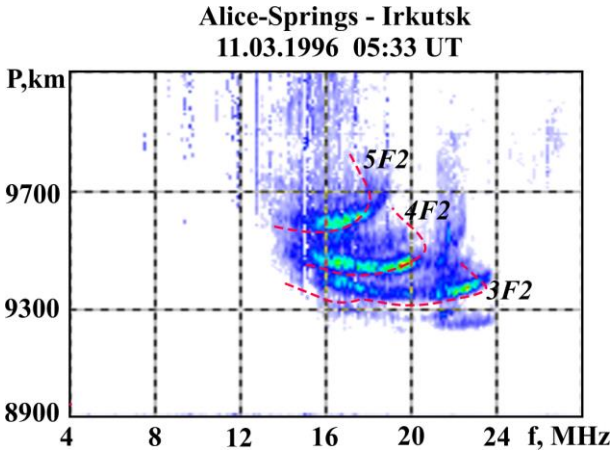

Figure 9. OS ionogram obtained from the Alice Springs—Irkutsk path on March 11, 1996 at 05:33 UT and the results of interpretation of propagation modes

CONCLUSION

We have described the method and algorithms for modeling HF radio paths of different lengths and orientation within the framework of the waveguide approach — the normal mode method.

- Numerical algorithms have been developed for calculating normal mode characteristics, taking into account the spectral parameter complexity;
- Algorithms have been developed for modeling distance-frequency, frequency-angular, and amplitude characteristics of signals over HF radio paths through analysis and numerical summation of a number of normal modes;
- We have implemented the comprehensive algorithm for modeling HF radio paths, which includes a medium model, algorithms for calculating signal characteristics, and automatic interpretation of ionograms;
- We have compared the results of the calculation of MUF and DFC of OS and experimental data on OS obtained from paths of different lengths and orientation. The method of automatic processing and interpretation of OS ionograms is used to analyze experimental ionograms and determine MUF of propagation modes along the radio path.

The results of the complex algorithm for calculating the HF propagation characteristics can be used as input parameters for analyzing and identifying distortions of recorded signals over real radio paths, as well as for determining ranges of optimal operating frequencies.

The work was financially supported by the Ministry of Science and Higher Education of the Russian Federation (Subsidy No. 075-GZ/Ts3569/278). The experimental data was obtained using the equipment of Shared Equipment Center «Angara» [http://ckp-rf.ru/ckp/3056/].

REFERENCES

Anderson S. Cognitive HF radar. *J. Eng*. 2019, vol. 2019, iss. 20, pp. 6772–6776. DOI: 10.1049/joe.2019.0537.

Anyutin A.P., Orlov Yu.I. Space-time geometrical theory of diffraction of frequency-modulated radio signals in a homogeneous dispersive medium. *J. Commun. Technol. Electron*. 1977, vol. 22, no. 10, pp. 2082–2090.

Avdeev V.B., Demin A.V., Kravtsov Yu.A., Tinin M.V., Yarygin A.P. The interferential integral method (review) *Radiophys Quantum Electron*. 1988, vol. 31, pp. 907–921.

Ayliffe J.K., Durbridge L.J., Gordon J.F., Gardiner-Garden R. The DST Group High-Fidelity, Multichannel Oblique Incidence Ionosonde. *Radio Sci*. 2019, vol. 54, no. 1, pp. 104–114. DOI: 10.1029/2018RS006681.

Baranov V.A., Karpenko A.L., Popov A.V. Evolution of Gaussian beams in the nonuniform Earth-ionosphere waveguide. *Radio Sci*. 1992, vol. 27, no. 2, pp. 307–314. DOI: 10.1029/91RS02639.

Baranov V.A., Popov A.V. Generalization of the parabolic equation for EM waves in a dielectric layer of nonuniform thickness. *Wave Motion*. 1993, vol. 17, no. 4, pp. 337–347. DOI: 10.1016/0165-2125(93)90013-6.

Bilitza D., Altadill D., Truhlik V., Shubin V., Galkin I., Reinisch B., Huang X. International Reference Ionosphere 2016: From ionospheric climate to real-time weather predictions. *Space Weather*. 2017, vol. 15, no.2, pp. 418–429. DOI: 10.1002/2016SW001593.

Bremmer H. *Terrestrial Radio Waves*. Theory of Propagation, Amsterdam, 1949, 343 p.

Cherkashin Yu.N. Application of parabolic equation method for calculation wavefields in inhomogeneous media *Radio Engineering and Electronic Physics*. 1971, vol. 16, no. 1, pp. 173–174. (In Russian).

Croft T.A., Hoogasian H. Exact ray calculations in a quasi-parabolic ionosphere with no magnetic field. *Radio Sci*. 1968, vol. 3, no. 1, pp. 69–74. DOI: 10.1002/rds19683169.

Davies K. *Ionospheric Radio Waves. Blaisdell*, London, 1969, 460 p.

Dyson P.L., Bennett J.A. A model of the vertical distribution of the electron concentration in the ionosphere and its application to oblique propagation studies. *J. Atmos. Terr. Phys*. 1988, vol. 50, no. 3, pp. 251–262. DOI: 10.1016/0021-9169(88)90074-8.

Grozov V.P., Ilyin N.V., Kotovich G.V., Ponomarchuk S.N. Software system for automatic interpretation of ionosphere sounding data. *Pattern Recognition and Image Analysis*. 2012, vol. 22, no. 3, pp. 458–463.

Gurevich A.V., Tsedilina E.E. *Long distance propagation of HF radio waves*. Berlin: Springer-Verlag. 1985.

Haselgrove J. Oblique ray paths in the ionosphere. *Proceedings of the Physical Society. Section B*. 1957, vol. 70, no. 7, pp. 653–662.

Ilyin N.V., Khakhinov V.V., Kurkin V.I., Nosov V.V., Orlov I.I., Ponomarchuk S.N. The theory of chirp-signal ionospheric sounding. *Proceedings of ISAP'96, Chiba, Japan*, 1996, pp. 689–692.

Ipatov E.B., Lukin D.S., Palkin E.A. Numerical realization of the Maslov canonical operator method for problems of shortwave radio propagation in the ionosphere of the earth. *Radiophysics and Quantum Electronics*. 1990, vol. 33, no. 5, pp. 411–420. DOI: 10.1007/BF01045406.

Ipatov E.B., Kryukovskii A.S., Lukin D.S., Palkin E.A., Rastyagaev D.V. Methods of simulation of electromagnetic wave propagation in the ionosphere with allowance for the distributions of the electron concentration and the Earth's magnetic field. *J. Commun. Technol. Electron*. 2014, vol. 59, no. 12, pp. 1341–1348. DOI: 10.1134/S1064226914120079.

Ivanov D.V., Ivanov V.A., Ovchinnikov V.V., Elsukov A. Adaptive wideband equalization for frequency dispersion correction in HF band considering variations in interference characteristics and ionosphere parameters. *ITM Web Conf*. 2019a, vol. 30, no. 15021, pp. 1–6. DOI: 10.1051/itmconf/20193015021.

Ivanov V.A., Ivanov D.V., Ryabova N.V., Ryabova M.I., Chernov A.A., Ovchinnikov V.V. Studying the parameters of frequency dispersion for radio links of different length using software-defined radio based sounding system. *Radio Sci.* 2019b, vol. 54, no. 1, pp. 34–43. DOI: 10.1029/2018RS006636.

Ivanov V.A., Kurkin V.I., Nosov V.E., Uryadov V.P., Shumaev V.V. Chirp ionosonde and its application in the ionospheric research. *Radiophysics and Quantum Electronics*. 2003, vol. 46, iss. 11, pp. 821–851.

Kazantsev A.N., Lukin D.S., Spiridonov Yu.G. A method for studying the propagation of radio waves in an inhomogeneous magnetoactive ionosphere. *Space Res.* 1967, vol. 5, no. 4, pp. 593–600. (In Russian).

Kelso J.M. Ray Tracing in the Ionosphere. *Radio Sci*. 1968, vol. 3, no. 1, pp. 1–12. DOI: 10.1002/rds1968311.

Krasnushkin P.E. *The method of normal waves as applied to the problem of long-distance radio communications*. Moscow: Publishing House of Moscow State University. 1947, 52 p. (In Russian).

Kravtsov Yu. A., Orlov Yu. I., Geometrical Optics of Inhomogeneous Media. *Springer, Berlin*. 1990.

Kryukovskii A.S., Lukin D.S., Palkin E.A., Rastyagaev D.V. Wave catastrophes: Types of focusing in diffraction and propagation of electromagnetic waves. *J. Commun. Technol. Electron*. 2006, vol. 51, no. 10, pp. 1087–1125. DOI: 10.1134/S1064226906100019.

Kurkin V.I., Orlov I.I., Popov V.N. Technique for calculating the MUF of long radio paths. *Research on geomagnetism, aeronomy and solar physics. Moscow: Nauka*. 1975, iss. 33, pp. 71–74. (In Russian).

Kurkin V.I., Orlov I.I., Popov V.N. *Normal Wave Technique in HF Radio Communication Problem*. Moscow, Nauka Publ., 1981a. (In Russian).

Kurkin V.I., Orlov I.I., Popov V.N. Use of the normal wave method in study of long-distance radio paths. *Radiophysics and Quantum Electronics*. 1981b, vol. 24, iss. 3, pp. 203–206. DOI: 10.1007/BF01035369.

Kurkin V.I., Orlov I.I., Potekhin A.P. On a technique for calculating the amplitude of a quasi-monochromatic HF signal in the normal-wave method. *Research on geomagnetism, aeronomy and solar physics. Moscow: Nauka*. 1982, iss. 59, pp. 60–62. (In Russian).

Kurkin V.I., Ilyin N.V., Penzin M.S., Ponomarchuk S.N., Khakhinov V.V. HF radio channel modeling on the base of waveguide approach. *Solar-Terr. Phys.* 2023, vol. 9, iss. 4, pp. 83–94. DOI: 10.12737/stp-94202311.

Kurkin V.I., Medvedeva I.V., Podlesnyi A.V. Effect of sudden stratosphere warming on characteristics of medium-scale traveling ionospheric disturbances in the Asian region of Russia. *Adv. Space Res*. 2024, vol. 73, iss. 7. P. 3613–3623. DOI: 10.1016/j.asr.2023.09.020.

Lukin D.S., Spiridonov Yu.G. Application of the method of characteristics for the numerical solution of problems of radio wave propagation in an inhomogeneous and nonlinear medium. *Radiotekhnika i Elektronika*. 1969, vol. 14, no. 9, pp. 1673–1677. (In Russian).

Mullaly R. F. Ray paths in inhomogeneous anisotropic media. *Australian Journal of Physics*. 1962, vol. 15, no. 2, pp. 96–105. DOI: 10.1071/PH620096.

Podlesnyi A.V., Brynko I.G., Kurkin V.I., Berezovsky V.A., Kiselyov A.M., Petukhov E.V. Multifunctional chirp ionosonde for monitoring the ionosphere. *Heliogeophys. Res.* 2013, no. 4, pp. 24–31. (In Russian).

Podlesnyi A.V., Lebedev V.P., Ilyin N.V., Khahinov V.V. Implementation of the method for restoring the transfer function of the ionospheric radio channel based on the results of sounding the ionosphere with a continuous chirp signal. *Electromagnetic waves and electronic systems*. 2014, vol. 19, no. 1, pp. 63–70. (In Russian).

Ponomarchuk S.N., Grozov V.P., Ilyin N.V., Kurkin V.I. Backscatter Ionospheric Sounding by a Continuous Chirp Signal. *Radiophysics and Quantum Electronics*. 2022, vol. 64, iss. 8-9, pp. 591–604. DOI: 10.1007/s11141-022-10162-7.

Ponomarchuk S.N., Grozov V.P. Automatic interpretation of ionograms of oblique sounding with a continuous chirp signal based on hybrid algorithms. *Proc. SPIE 12780, 29th International Symposium on Atmospheric and Ocean Optics: Atmospheric Physics*, 127806R (17 October 2023). DOI: 10.1117/12.2688445.

Popov V.N., Potekhin A.P. On the propagation of decameter radio waves in the azimuth-symmetric "Earth-ionosphere" waveguide. *Research on geomagnetism, aeronomy and solar physics. Moscow: Nauka*. 1984, iss. 69, pp. 9–15. (In Russian).

Potekhin A.P., Orlov I.I. An approximate summation formula for a series of normal waves. *Research on geomagnetism, aeronomy and solar physics. Moscow: Nauka*. 1981, iss. 57, pp. 135–137. (In Russian).

Rao N.N. Bearing deviation in HF transionospheric propagation. I. Exact computations for some ionospheric models with no magnetic field. *Radio Sci*. 1968. vol. 3, no. 12, pp. 1113–1118. DOI: 10.1002/rds19683121113.

Zernov N.N., Gherm V.E., Zaalov N.Yu., Nikitin A.V. The generalization of Rytov's method to the case of inhomogeneous media and HF propagation and scattering in the ionosphere. *Radio Sci*. 1992, vol. 27, no. 2, pp. 235–244. DOI: 10.1029/91rs02920.

URL: http://ckp-rf.ru/ckp/3056/ (accessed January 31, 2024).

Original Russian version: Ponomarchuk S.N., Kurkin V.I., Ilyin N.V., Penzin M.S., published in Solnechno-zemnaya fizika. 2024. Vol. 10. Iss. 2. P. 99–108. DOI: 10.12737/szf-102202409.

How to cite this article

Ponomarchuk S.N., Kurkin V.I., Ilyin N.V., Penzin M.S. HF radio path modeling by waveguide approach. *Solar-Terrestrial Physics.* 2024. Vol. 10. Iss. 2. P. 93–101. DOI: 10.12737/stp-102202409.